

1 **Different B cell subpopulations show distinct patterns in their IgH repertoire metrics**

2
3 Marie Ghraichy¹, Valentin von Niederhäusern¹, Aleksandr Kovaltsuk², Jacob D. Galson^{1,3},
4 Charlotte M. Deane², Johannes Trück¹

5
6 *¹ Division of Immunology, University Children's Hospital and Children's Research Center,
7 University of Zurich (UZH), Switzerland*

8 *² Department of Statistics, University of Oxford, United Kingdom*

9 *³ Alchemab Therapeutics Ltd, London, United Kingdom*

10

11 **Abstract**

12 *Background:*

13 Several human B-cell subpopulations are recognized in the peripheral blood, which play
14 distinct roles in the humoral immune response. These cells undergo developmental and
15 maturational changes involving VDJ recombination, somatic hypermutation and class switch
16 recombination, altogether shaping their immunoglobulin heavy chain (IgH) repertoire.

17 *Methods:*

18 Here, we sequenced the IgH repertoire of naïve, marginal zone, switched and plasma cells
19 from 10 healthy adults along with matched unsorted and *in silico* separated CD19⁺ bulk B
20 cells. We used advanced bioinformatic analysis and machine learning to thoroughly examine
21 and compare these repertoires.

22 *Results:*

23 We show that sorted B cell subpopulations are characterised by distinct repertoire
24 characteristics on both the individual sequence and the repertoire level. Sorted subpopulations
25 shared similar repertoire characteristics with their corresponding *in silico* separated subsets.
26 Furthermore, certain IgH repertoire characteristics correlated with the position of the constant
27 region on the IgH locus.

28 *Conclusion:*

29 Overall, this study provides unprecedented insight over mechanisms of B cell repertoire
30 control in peripherally circulating B cell subpopulations.

31 **Introduction**

32 B-cell development starts in the bone marrow where immature B cells must assemble and
33 express on their surface a functional but non-self-reactive B cell antigen receptor (BCR).¹ The
34 generation of the heavy and light chain of the BCR is mediated by the random and imprecise
35 process of V(D)J recombination.² Further development of B cells occurs in the periphery in
36 response to stimulation with the process of somatic hypermutation (SHM) through which point
37 mutations are introduced in the genes coding for the V(D)J part of the immunoglobulin heavy
38 (IgH) and light chain.³ Subsequently, B cells with a mutated BCR providing increased antigen
39 affinity are selected and show increased survival and proliferation capacity.⁴

40 Furthermore, class-switch recombination (CSR) modifies the IgH constant region resulting in
41 the generation of B cells with nine different immunoglobulin isotypes or isotype subclasses,
42 namely IgD, IgM, IgG1-4, IgA1/2 and IgE.⁵ This process involves the replacement of the
43 proximal heavy chain constant gene by a more distal gene. Class switching is an essential
44 mechanism during humoral immune responses as the constant region of an antibody determines
45 its effector function.⁶ Both direct switching and sequential switching upon a second round of
46 antigen exposure have been reported.⁷⁻⁹

47
48 Through developmental mechanisms and further differentiation in the periphery, several
49 phenotypically distinct circulating B cell subpopulations are generated.¹⁰ They include naïve,
50 marginal zone (MZ), switched memory B cells and plasma cells (PC), which are mainly
51 characterized by their differential expression of surface markers and by playing distinct roles
52 in the adaptive immune response.¹¹ High-throughput sequencing of the IgH repertoire (AIRR-
53 seq) has made it possible to improve our understanding of the different components of the
54 adaptive immune system in health and disease, and following vaccine challenge.¹²⁻¹⁶ Previous
55 studies using both high- and low-throughput sequencing techniques have already reported
56 important differences between B-cell subpopulations affecting their IgH repertoire
57 composition, VDJ gene usage, mutations and clonality.¹⁷⁻²⁰

58
59 Recent AIRR-seq workflows allow coverage of a sufficient part of the IgH constant region in
60 addition to the VDJ region, making it possible to assign antibody classes and subclasses on an
61 individual sequence level. It is common practice to use unsorted bulk B cells from peripheral
62 blood as a starting material and use the constant region information combined with the degree
63 of SHM to group transcripts *in silico* into different B cell populations.^{21,22} Using isotype-
64 resolved IgH sequencing of bulk B cells, isotype subclasses have been found to show
65 differences in their repertoire characteristics.^{23,24} However, it remains unknown how the IgH
66 repertoire of bioinformatically separated transcripts originating from bulk-sequenced B cells
67 compares to the repertoire of their corresponding circulating B cell subpopulations. It is also
68 unknown how IgH sequences with the same constant region originating from different cell types
69 compare.

70
71 Here, we used an established AIRR-seq workflow that captures the diversity of the variable IgH
72 genes together with the isotype subclass usage to study in detail the repertoire of CD19⁺ bulk
73 B cells as well as flow cytometry sorted naïve, MZ, switched and plasma cells from 10 healthy
74 adults. We applied advanced statistical methods and machine learning algorithms to combine
75 several repertoire metrics and characterize the different B cell subpopulations. We show that
76 transcripts from physically sorted B cell subpopulations share similar characteristics with their
77 corresponding subsets in the bulk that were grouped *in silico* using isotype subclass information
78 and number of mutations. We further demonstrate that sequences with the same isotype
79 subclass originating from different cell types are closely related, suggesting the presence of
80 isotype-specific rather than cell-type specific signatures in the IgH repertoire. We finally
81

82 correlate these signatures to the isotype subclass positioning on the locus and find that
83 downstream subclasses exhibit enhanced signs of maturity, overall providing new insights into
84 the selection and the peripheral differentiation of distinct B cell subpopulations.

85

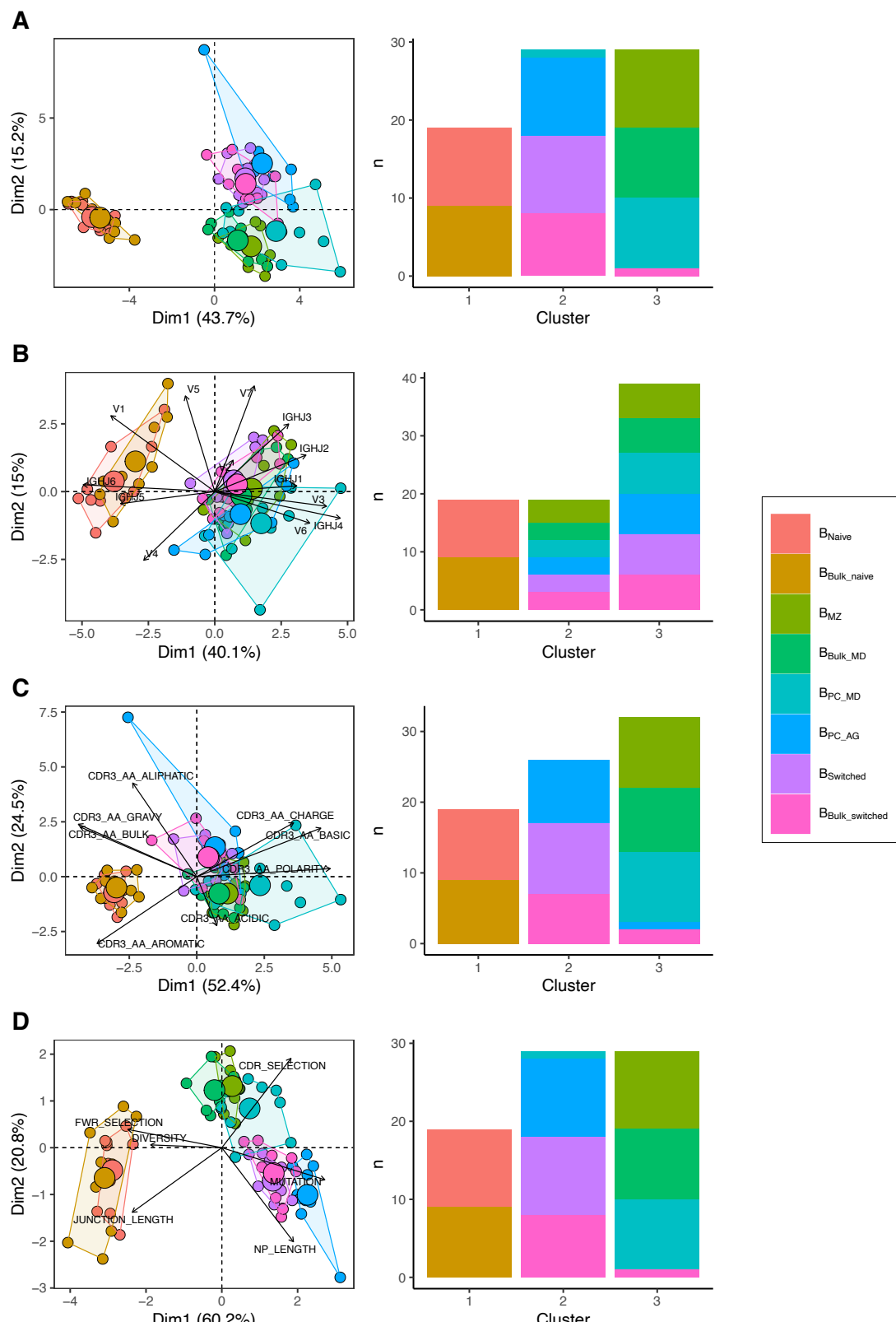
86 **Results**

87

88 **Physically sorted B cell subpopulations and their corresponding subsets in the bulk share 89 similar repertoire characteristics**

90 We compared IgH repertoire characteristics between the following B cell subpopulations:
91 B_{naive} , B_{MZ} , $B_{\text{PC_MD}}$, $B_{\text{PC_AG}}$, and B_{switched} and their corresponding subsets that we obtained *in*
92 *silico* from B_{bulk} : $B_{\text{bulk_naive}}$, $B_{\text{bulk_MD}}$, and $B_{\text{bulk_switched}}$. We identified three separate clusters: one
93 made of predominantly B_{MZ} , $B_{\text{bulk_MD}}$ and $B_{\text{PC_MD}}$; another with only B_{naive} and $B_{\text{bulk_naive}}$; and a
94 third cluster with predominantly $B_{\text{bulk_switched}}$, $B_{\text{PC_AG}}$ and B_{switched} (*Figure 1A*) by combining all
95 repertoire characteristics in a PCA and applying k-means clustering. To test whether this
96 clustering pattern was driven by VJ gene usage, CDR3 physiochemical properties or the general
97 repertoire metrics, we analysed these variables separately. Using V family and J gene usage,
98 there was a clear separation between naïve and memory cells mostly driven by differences in
99 V1/3 and J4/6 usage (*Supplementary figure 1*). However, no separation between $B_{\text{MZ}}/B_{\text{PC_MD}}$ /
100 $B_{\text{bulk_MD}}$ and $B_{\text{switched}}/B_{\text{PC_AG}}/B_{\text{bulk_switched}}$ was observed (*Figure 1B*). The CDR3 physiochemical
101 properties alone created similar clusters as when combined together with the other metrics
102 (*Figure 1C*). This separation was mostly driven by a lower basic and a higher aromatic content
103 in addition to a higher gravy index and a lower polarity in $B_{\text{naive}}/B_{\text{bulk_naive}}$ compared to memory
104 subpopulations (*Supplementary figure 2*). Global repertoire metrics also created a clear
105 separation between $B_{\text{naive}}/B_{\text{bulk_naive}}$, $B_{\text{switched}}/B_{\text{PC_AG}}/B_{\text{bulk_switched}}$ and $B_{\text{MZ}}/B_{\text{PC_MD}}/B_{\text{bulk_MD}}$
106 subpopulations mostly driven by higher mutation counts, NP length and selection pressure in
107 the CDR and lower junction length and diversity in B_{switched} compared to B_{naive} (*Supplementary
108 figure 3*).

109 In summary, we found that V family and J gene usage, the physiochemical properties of the
110 CDR3, and global repertoire metrics similarly distinguish between B cell subpopulations: B_{naive} ,
111 $B_{\text{MZ}}/B_{\text{PC_MD}}$ and $B_{\text{switched}}/B_{\text{PC_AG}}$ were divergent but shared properties with their relative
112 corresponding subsets in the bulk.



113

114

115

116

117

118

119

120

Figure 1: Different repertoire characteristics similarly separate between B cells subpopulations. PCA (left) and composition of the clusters formed using k-means clustering with k=3 (right) applied on A) all repertoire characteristics, B) V family and J gene usage, C) physiochemical properties of CDR3 junction, D) global repertoire metrics. The percentage of all variation in the data that is explained by PC1 and PC2 is shown on the x and y axis respectively between brackets. In the PCA plots, areas are the convex hulls of the subsets and the largest point of one color represents the center of that hull.

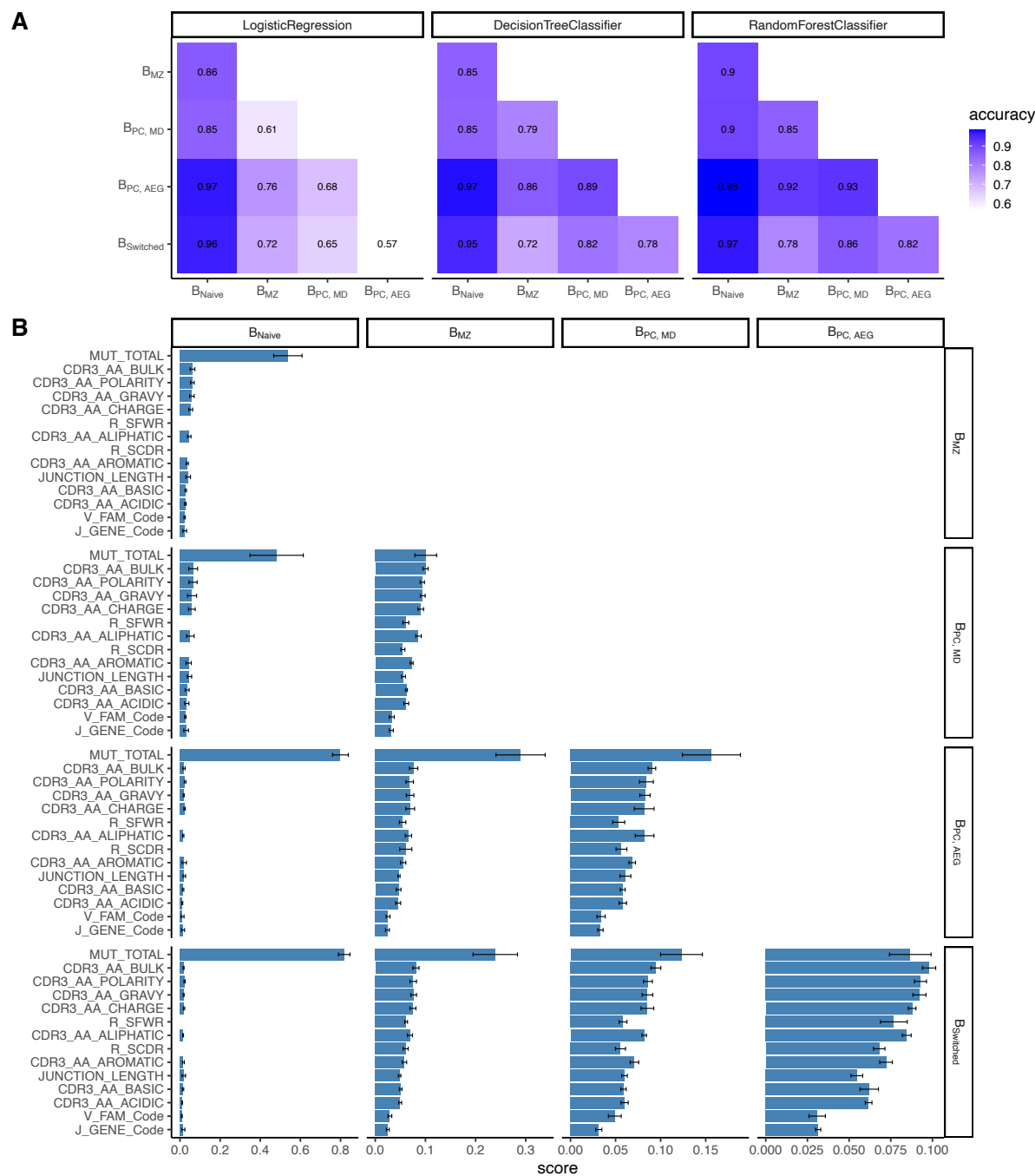
121 **Accurate prediction of cell type based on repertoire features on a single-cell level**

122 We constructed a sequence classifier that predicts the cell type of a sequence using sequence
123 attributes and different repertoire metrics. Since we subsampled our data making our datasets
124 perfectly balanced, we used only accuracy as a performance metric. Logistic regression,
125 decision tree and random forest classifiers all performed satisfactorily (*Figure 2A*). However,
126 logistic regression performed poorly on correctly classifying B_{switched} and $B_{\text{PC_AG}}$, for which
127 accuracy was almost equal to chance. The performance of all three classifiers was highest in
128 distinguishing between B_{naive} and other cell types.

129 The random forest classifier was the most successful compared to the other two and the most
130 accurate in predicting the cell type of a sequence. We assessed the relevance of specific
131 predictors in properly classifying cell types by calculating feature importance scores for each
132 cell pair (*Figure 2B*). The number of mutations was the highest scoring feature for all cell pairs
133 except for distinguishing between B_{switched} and $B_{\text{PC_AG}}$ and between B_{MZ} and $B_{\text{PC_MD}}$ for which
134 CDR3 amino acid characteristics had higher scores. Within the CDR3 physiochemical
135 properties, average bulkiness, average polarity and the gravy hydrophobicity index were the
136 most differentiating between cell types whereas the basic and acidic content of the CDR3 chain
137 seemed to be less important. R/S ratio in CDR and FWR and the junction length appeared to
138 have similar scores and were more important in cases where B_{naive} were not one of the two cell
139 types. V family and J gene appeared to have low importance in distinguishing between all cell
140 pairs.

141

142



143

144

Figure 2: Classification accuracies and feature scores on a single-sequence level. A)

145 Heatmap showing pairwise classification accuracy results using logistic regression, decision
146 tree and random forest classifier. B) Random forest feature scores by cell pair.

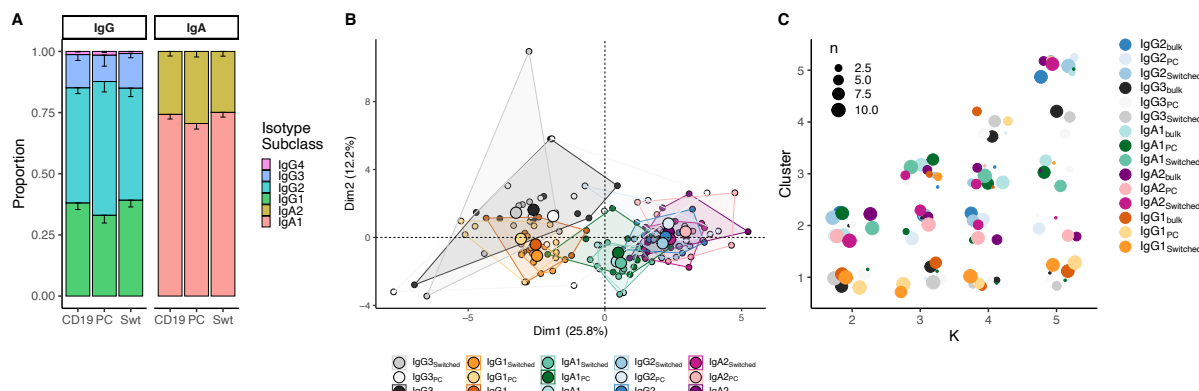
147

148 **Within class switched subsets, sequences with same constant region from different cell
149 types show similar features.**

150 When comparing class-switched transcripts originating from B_{bulk}_switched, B_{switched}, and B_{PC}_AG,
151 isotype subclasses were similarly distributed: IgA1 was the dominant subclass in IgA
152 transcripts whereas IgA2 was less frequently used. All cells showed a dominant use of IgG1
153 and IgG2 with little IgG3 and negligible IgG4 (*Figure 3A*). Usage of IgA1 in B_{PC}_AG was similar
154 to B_{switched} and B_{bulk}_switched ($p=0.28$ and $p=0.25$, Kruskal-Wallis). IgG3 usage was significantly
155 lower in B_{PC}_AG compared to B_{bulk}_switched and B_{switched} ($p=0.01$, $p=0.01$, Kruskal-Wallis) while
156 IgG1 usage tended to be lower ($p=0.13$ and $p=0.11$, Kruskal-Wallis) and IgG2 usage higher in
157 B_{PC}_AG compared to the other two B cell subpopulations ($p=0.11$ and $p=0.11$, Kruskal-Wallis).

158 When combining repertoire characteristics by isotype subclass and cell type for class-switched
 159 transcripts resulting from $B_{bulk_switched}$, $B_{switched}$ and B_{PC_AG} , we found that samples with the same
 160 constant region originating from different cell types overlapped. (Figure 3B) We identified two
 161 clusters: one mainly composed of IgG1 and IgG3 samples from all cell types and another with
 162 IgA1, IgA2 and IgG2 samples by applying k-means clustering with $k=2$ (Figure 3C). By further
 163 dividing the data and with increasing k , we observed that newly formed clusters were mainly
 164 composed of distinct isotype subclasses, while the cell type itself was not a defining factor for
 165 cluster formation. Interestingly, we couldn't see a clear separation between IgG2 and IgA2
 166 samples with increasing number of clusters.

167
 168



169
 170 **Figure 3: Analysis of isotype subclasses in IgG and IgA transcripts.** A) Isotype subclass
 171 distribution by cell type. Error bars represent the standard error of the mean. B) PCA on all
 172 repertoire properties combined by cell type and isotype subclass. Areas are the convex hulls of
 173 a group and the largest point of one color represents the center of that hull. C) Composition of
 174 the clusters formed by applying the k-means clustering algorithm on all data with increasing k
 175 from $k=2$ to $k=5$

176

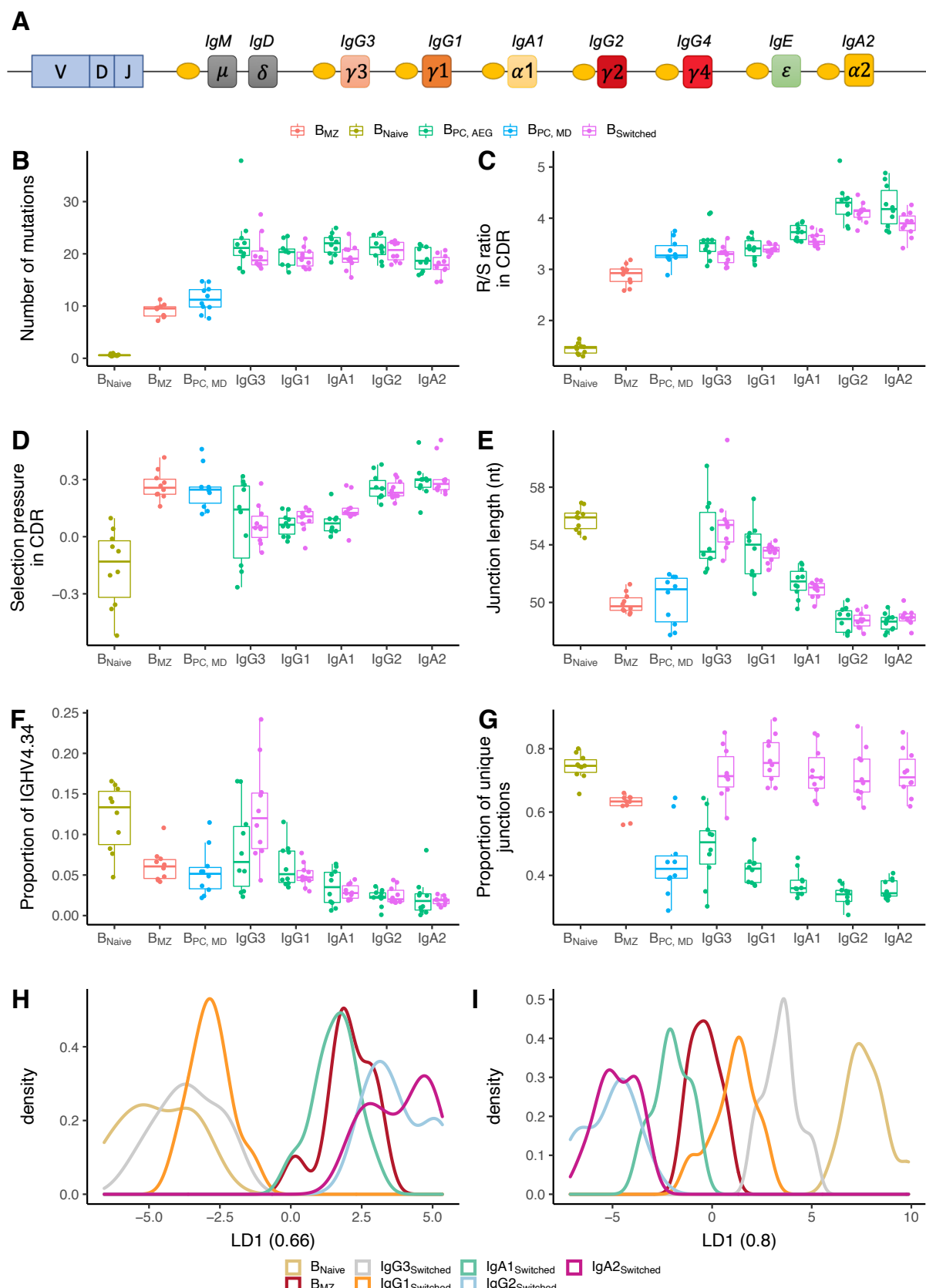
177 **B cell repertoire metrics correlate with constant region positioning on the IgH locus.**

178 The IgH locus contains 9 constant genes: the genes encoding for IgM and IgD are the closest
 179 to the V-D-J recombination sites while those for IgG3, IgG1 and IgA1 are further downstream
 180 but still close to IgM/IgD whereas more distant on the locus are the genes that encode for IgG2,
 181 IgG4, IgE and IgA2 (Figure 4A). We determined and compared B cell repertoire metrics
 182 between different subclasses in B_{PC} and $B_{switched}$ and compared those to B_{naive} and B_{MZ} . B_{naive}
 183 showed the lowest number of mutations and R/S ratio and longest CDR3 junction. Memory
 184 subsets had a high number of mutations, with B_{MZ} and B_{PC_MD} having fewer mutations than
 185 class switched transcripts (Figure 4B). IgM-distal subclasses IgG2 and IgA2 in both $B_{switched}$
 186 and B_{PC_AG} showed the highest R/S ratio indicating high selection pressure (Figure 4C). All
 187 antigen-experienced subsets had a lower junction length compared to B_{naive} except for IgM-
 188 proximal transcripts IgG3 and IgG1 (Figure 4E). The proportion of IGHV4-34, the gene
 189 associated with self-reactivity³³, was lower in memory subsets compared to B_{naive} except for
 190 IgG3 from $B_{switched}$ for which the proportion of IGHV4-34 was similar to naïve subsets (Figure
 191 4F). Within IgG and IgA sequences, genomic distance from IgM correlated with a higher R/S
 192 ratio, shorter junction and lower usage of IGHV4-34. B_{PC} had a significantly lower diversity
 193 compared to all other cell types (Figure 4G). Interestingly, transcripts from $B_{switched}$ showed a
 194 similar diversity to B_{naive} whereas B_{MZ} were less diverse. Within B_{PC_AG} , IgM-distal subclasses
 195 showed a lower diversity.

196 IGHV family andIGHJ gene usage also showed a discrepancy between different subsets: IGHV
 197 family usage in IgM-proximal subclasses IgG3 and IgG1 was similar to B_{Naive} . B_{MZ} and IgM-
 198 distal subclasses were enriched in IGHJ4 at the expense of IGHJ6 compared to naïve cells and

199 IgG1-3 B-cell subsets (*Supplementary figure 4*). To reduce the dimensionality of all data points
200 into a single one-dimensional axis, we performed LDA fitted on the relative gene frequencies
201 (*Figure 4H*). This showed a clear distinction between B_{naive} , IgG1-3 and B_{MZ} , IgG2 and IgA1-
202 2. An LDA fitted on the physiochemical properties of the CDR3 junction also showed a clear
203 distinction between naïve and memory subsets, with IgG3 and IgG1 being closest to B_{naive} and
204 IgG2 and IgA2 overlapping and furthest away (*Figure 4I*).
205

206 In summary, we found that different B cell repertoire metrics correlate with the positioning of
207 their respective subclass genes on the IgH locus, namely with the increasing genomic distance
208 from IgM, with the proximal IgH subclasses being more similar to naïve.
209



210
211
212
213
214
215

Figure 4: Analysis of repertoire metrics by isotype subclass and cell type. A) Overview of the IgH constant region locus. Comparison of A) mutation counts, B) R/S ratio, C) selection pressure, D) junction length, F) proportion of IGHV4-34 and G) diversity between different B cell subpopulations. LDA fitted on H) V family and J gene usage and I) CDR3 amino acid physiochemical properties.

216 **Discussion**

217
218 Here, we used AIRR-seq to characterize similarities and differences in the IgH repertoire of
219 bulk B cells and different sorted naïve and memory B cell populations. This allowed for an in-
220 depth understanding of the mechanisms underlying B-cell responses. We report differences in
221 V family and J gene usage, CDR3 physiochemical properties and global repertoire
222 characteristics that similarly distinguish between naïve, IgM/IgD memory and class switched
223 subsets both at the repertoire and at the sequence level. Furthermore, we show differences in
224 the repertoire characteristics at the isotype subclass level unrelated to cell type that correlate
225 with the position of the constant gene on the IgH locus. This study provides powerful insight
226 on biological mechanisms underlying the B cell response as well as novel understanding of
227 AIRR-seq methodologies to be taken into account in future studies.
228

229 Previous work involving human naïve and antigen-experienced B cell repertoires have shown
230 naïve B cells to have shorter junctions and higher usage of IGHJ6 and IGHV3, and lower usage
231 of IGHJ4 and IGHV1 compared with IgM memory and switched B cells.³⁴⁻³⁷ Differences in
232 gene usage and CDR3 properties between IgM memory and switched B cells have also been
233 reported.²⁰ IgM memory and switched B cells have been found to use more negatively charged
234 residues and to have less hydrophobic junctions compared with naïve B cells.^{18,20} Here, we
235 focused on a more detailed examination of the repertoires by combining multiple characteristics
236 using dimensionality reduction methods. Results of a previous study revealed that combining
237 only a few repertoire characteristics is sufficient to discriminate between B cell
238 subpopulations.¹⁹ In addition, an LDA combining V gene family proportions has been found to
239 successfully distinguish between IgM and IgG repertoires.³⁸ We extend these findings by
240 showing that using V family and J gene usage, CDR3 physiochemical properties or global
241 repertoire characteristics similarly allow to separate between naïve and memory
242 subpopulations. This suggests that distinct B cell subpopulations derive from different
243 developmental mechanisms and are subject to selective processes that lead to similar variable
244 gene identity. This can also reflect that different types of B cells are stimulated by different
245 types of antigens and therefore have distinctive junction compositions and properties.
246

247 Previous research has demonstrated that same B cell subpopulations from different donors are
248 more similar in their repertoire characteristics than different B cell subpopulations within an
249 individual.^{39,40} This has led to the understanding that differences between naïve and memory
250 cells are conserved across unrelated individuals. Our findings are in agreement with these
251 observations, and we extend on those by showing that the main defining factor in repertoire
252 similarity is the constant region type, namely the isotype subclass, and that differences between
253 subclasses are conserved across both cell type and individual. This finding suggests the
254 existence of an isotype-based mechanism for repertoire control that is constant across cell types
255 and individuals.
256

257 In addition to the comparative analysis of the different peripheral B cell subsets, our study
258 represents, to our knowledge, the first comparison of bulk B cell sequencing with sorted B cell
259 subpopulations. We showed that sequencing unsorted B cells from peripheral blood and
260 combining the constant region information with the degree of SHM to bioinformatically group
261 transcripts yields accurate results comparable to physical sorting, especially when analysing
262 global repertoire characteristics. We acknowledge that this might be limiting in tasks sensitive
263 to potential biases from different RNA levels per cell such as identifying antigen-specific
264 sequences from plasma cells.
265

266 Recent IgH repertoire studies have moved towards using machine learning and artificial
267 intelligence in contrast to traditional statistical approaches for goals including vaccine design,
268 immunodiagnostics and antibody discovery.⁴¹⁻⁴⁴ Previous work has focused on representing
269 repertoires as sequence or subsequence-based features, i.e. overlapping amino acid k-mers and
270 their Atchley biophysicochemical properties.^{41,42} Here, we report a simple pairwise classifier
271 that successfully predicts the cell type of a sequence based on only the commonly used sequence
272 attributes such as number of mutations and junction length. Random forest and decision tree
273 classifiers outperformed the logistic regression algorithm suggesting a non-linear separation
274 between cell types. A common concern when applying machine learning is the possibility of
275 over-fitting. To prevent this, we trained the algorithm on 80% of the data and tested its
276 performance on the remaining unseen 20%. We also subsampled every pair of classes to equal
277 number of sequences in order to balance the dataset. The model presented here is applied only
278 within an individual and is thereby confined by repertoire signals that might be individual-
279 specific. More work improving the generalisability of the model across individuals would be
280 revolutionizing in terms of its potential practical applications. Unsurprisingly, the number of
281 mutations was the most important feature in distinguishing between cell types. These results
282 along with previous work are promising and suggest that increasing the predictive potential of
283 machine learning methods could help in finding sequence characteristics that distinguish
284 between groups, such as disease state and healthy.

285
286 Studies indicate that both direct and sequential CSR to IgM distal isotype subclasses can
287 occur.^{45,46} Several studies have provided evidence for sequential CSR. IgM was found to
288 commonly switch to proximal subclasses (IgG1, IgA1, and IgG2), but direct switches from IgM
289 to more downstream subclasses (IgG4, IgE, or IgA2) were rare.⁷ It has also been reported that
290 a deficiency in IgG3, the most IgM-proximal subclass, frequently results in a decrease in other
291 IgG subclasses.⁴⁷ Although it is challenging to determine whether sequential CSR occurs during
292 a primary response, by re-entry into the germinal center, or during a secondary response to the
293 same antigen, we and others have shown that IgM-distal subclasses accumulate with age, likely
294 due to secondary encounter with antigen.^{22,48} Studies comparing the mean mutation number
295 between isotype subclasses have shown contradicting results: in one study, mutations varied in
296 relation to the constant region position on the IgH locus, with the closest to IgM (IgG3) having
297 the lowest mutations,²³ while in another study, no such difference was observed.²⁴ We didn't
298 find a difference in number of mutations among IgG subclasses. Our findings rather suggest
299 that mutation is more efficient in more downstream subclasses as we found that these exhibit
300 higher R/S ratios and selection pressure in the CDR, consistent with previous studies.⁴⁹
301 Generally, IgM distal subclasses showed signs of maturity (shorter junctions, lowerIGHV4-34
302 usage) while transcripts from IgM proximal subclasses were more similar to those of naïve B
303 cells. These results suggest that sequential CSR subjects B cells to selective forces leading to
304 more mature variable gene properties without necessarily accumulating more mutations.

305
306 In summary, in this study we took an extensive look at the IgH repertoire of different flow
307 cytometry sorted as well as bioinformatically grouped cell types and isotype subclasses of
308 healthy individuals. Using advanced bioinformatic tools, statistical analysis and machine
309 learning, this analysis provides deep insight into the different mechanisms of B cell
310 development and boosts our understanding of the B cell system components in health.

311
312

313 **Material and methods**

314

315 **1. Sample collection and cell sorting**

316 Buffy coat samples were obtained from 10 anonymous healthy adults, hence no approval from
317 the local ethics committee was necessary. B cells were first isolated by magnetic cell sorting
318 using the human CD19 MicroBeads (Miltenyi Biotec, San Diego, CA) and the AutoMACS
319 magnetic cell separator. From 9 out of the 10 samples, 3×10^6 bulk CD19⁺ B cells (B_{bulk}) were
320 lysed and stored at -80C. The remaining cells were sorted by flow cytometry into 4
321 subpopulations using cell surface markers characteristic for naïve (B_{naive}), marginal zone (B_{MZ}),
322 plasma cells (B_{PC}), and switched memory B cells (B_{switched}). Cells were then lysed and stored at
323 -80C. Surface markers, demographics, number of cells and purity of each sample are outlined
324 in *supplementary table 1*.

325

326 **2. RNA extraction and library preparation**

327 RNA extraction was performed on the lysate using the RNeasy Mini Kit (Qiagen, Hilden,
328 Germany). Libraries were prepared as previously described.²² Briefly, two reverse transcription
329 (RT) reactions were carried out for each RNA sample resulting from B_{bulk} or B_{PC}: one with
330 equal concentrations of IgM and IgD specific primers and another with IgA, IgG, and IgE
331 specific primers. Only one RT reaction with IgM and IgD specific primers was performed on
332 B_{naive} and B_{MZ} samples; similarly, we applied one RT reaction with IgA, IgG and IgE primers
333 on samples obtained from B_{switched}. IgH cDNA rearrangements were then amplified in a two-
334 round multiplex PCR using a mix of IGHV region forward primers and Illumina adapter
335 primers, followed by gel extraction for purification and size selection. The final concentration
336 of PCR products was measured using Qubit prior to library preparation and combined with a
337 total of 12 equally concentrated samples. Final libraries barcoded with individual i7 and i5
338 adapters were sequenced in each run on the Illumina MiSeq platform (2x300bp protocol).

339

340 **3. Data preprocessing**

341 Preprocessing of raw sequences was carried out using the Immcantation toolkit and as per
342 Ghraichy et al 2020.^{22,25,26} Briefly, samples were demultiplexed based on their Illumina tags. A
343 quality filter was applied, paired reads were joined and then collapsed according to their unique
344 molecular identifier (UMI). Identical reads with different UMI were further collapsed resulting
345 in a dataset of unique sequences. VDJ gene assignment was carried out using IgBlast.²⁷ Isotype
346 subclass annotation was carried out by mapping constant regions to germline sequences using
347 stampy.²⁸ The number and type of V gene mutations was determined as the number of
348 mismatches with the germline sequence using the R package shazam.²⁶ The R package
349 alakazam was also used to calculate the physicochemical properties of the CDR3 amino acid
350 sequences.²⁶ Selection pressure was calculated using BASELINE and the statistical framework
351 used to test for selection was CDR_R/(CDR_R + CDR_S)²⁹.

352

353 **4. In silico grouping of sequences**

354 For B_{bulk} samples, we used the constant region information combined with the mutation counts
355 to classify individual sequences into different subsets: IgD and IgM sequences with up to 2 nt
356 mutations across the entire V gene were considered “unmutated” (B_{bulk_naive}) to account for
357 remaining PCR and sequencing bias. The remaining mutated IgD and IgM sequences were
358 labelled as IgD/IgM memory (B_{bulk_MD}). All class-switched sequences were defined as antigen-
359 experienced regardless of their V gene mutation count (B_{bulk_switched}). We split the sequences
360 originating from B_{PC} into two categories: IgM/IgD B_{PC} (B_{PC_MD}) and switched IgG/IgA PCs
361 (B_{PC_AG}) according to the constant region of the sequences.

362

363

364

5. Summarising repertoire characteristics

365 366 367 368 369

V family and J gene usage was calculated in proportions for each individual and cell type. We summarised the mean of the following CDR3 physiochemical characteristics: hydrophobicity, bulkiness, polarity, normalized aliphatic index, normalized net charge, acidic side chain residue content, basic side chain residue content, aromatic side chain content by individual and cell type.

370 371 372 373 374

Mean junction length, number of mutations, and numbers of non-template (N) and palindromic (P) nucleotide added at the junction were calculated by individual and cell type. Selection pressure was summarised separately in complementarity-determining region (CDR) and framework region (FWR). Diversity was calculated as the proportion of unique junctions out of total transcripts. The preceding characteristics are referred to as global repertoire metrics.

375

6. Dimensionality reduction and clustering

376 377 378 379 380

Principal component analysis (PCA) and k-means clustering were applied to the different repertoire characteristics to explore and find associations in the data. They were applied using the internal R functions prcomp() and kmeans().³⁰ Linear discriminant analysis (LDA) was performed using the R function lda() from the package MASS³¹.

381

7. Sequence classifier

382 383 384 385 386 387 388 389 390 391 392 393 394

We constructed the sequence classifier using the sklearn package in python³². Because we have the constant region information and to avoid error accumulation, we performed a pairwise classification thereby transforming the multiclass problem into a binary classification. Within every participant and for every pair of cells, we subsampled to the lower sequence number to avoid bias and dataset imbalance. We used the number of mutations, the physiochemical properties, and the junction length as numerical input features. The V gene family and J gene were one-hot encoded. In the case where the naïve cells were not one of the two classes, the replacement/silent (R/S) mutation ratios in CDR and FWR were included as features. We split the data into training and testing set using the default test size of 0.2. We used logistic regression, decision tree, and random forest classifiers for prediction. The accuracy was recorded to judge the overall performance of the models. For every pair of classes, the mean accuracy of the 10 samples was calculated.

395

8. Data Availability

396 397 398 399 400 401

Raw data used in this study are available at the NCBI Sequencing Read Archive (www.ncbi.nlm.nih.gov/sra) under BioProject number PRJNA748239 including metadata meeting MiAIRR standards (32). The processed dataset is available in Zenodo (<https://doi.org/10.5281/zenodo.3585046>) along with the protocol describing the exact processing steps with the software tools and version numbers.

402

403

Competing interests

404 405

None of the authors have declared any conflict of interest related to this work.

406 **References**

- 407 1. Lefranc, M.-P. & Lefranc, G. *The immunoglobulin factsbook*. Academic Press (2001).
- 408 2. Tonegawa, S. Somatic generation of antibody diversity. *Nature* **302**, 575–581 (1983).
- 409 3. Jolly, C. J. *et al.* The targeting of somatic hypermutation. *Semin. Immunol.* (1996).
410 doi:10.1006/smim.1996.0020
- 411 4. Zheng, N. Y., Wilson, K., Jared, M. & Wilson, P. C. Intricate targeting of
412 immunoglobulin somatic hypermutation maximizes the efficiency of affinity
413 maturation. *J. Exp. Med.* (2005). doi:10.1084/jem.20042483
- 414 5. Stavnezer, J., Guikema, J. E. J. & Schrader, C. E. Mechanism and Regulation of Class
415 Switch Recombination. *Annu. Rev. Immunol.* (2008).
416 doi:10.1146/annurev.immunol.26.021607.090248
- 417 6. Vidarsson, G., Dekkers, G. & Rispens, T. IgG subclasses and allotypes: From structure
418 to effector functions. *Front. Immunol.* **5**, 520 (2014).
- 419 7. Horns, F. *et al.* Lineage tracing of human B cells reveals the in vivo landscape of
420 human antibody class switching. *Elife* (2016). doi:10.7554/elife.16578
- 421 8. Cameron, L. *et al.* SeS μ and SeSy Switch Circles in Human Nasal Mucosa Following Ex
422 Vivo Allergen Challenge: Evidence for Direct as Well as Sequential Class Switch
423 Recombination. *J. Immunol.* (2003). doi:10.4049/jimmunol.171.7.3816
- 424 9. Zhang, K., Mills, F. C. & Saxon, A. Switch circles from IL-4-directed ϵ class switching
425 from human B lymphocytes: Evidence for direct, sequential, and multiple step
426 sequential switch from μ to ϵ Ig heavy chain gene. *J. Immunol.* (1994).
- 427 10. Allman, D. & Pillai, S. Peripheral B cell subsets. *Current Opinion in Immunology* (2008).
428 doi:10.1016/j.co.2008.03.014
- 429 11. Leandro, M. J. B-cell subpopulations in humans and their differential susceptibility to
430 depletion with anti-CD20 monoclonal antibodies. *Arthritis Research and Therapy*
431 (2013). doi:10.1186/ar3908
- 432 12. Mandric, I. *et al.* Profiling immunoglobulin repertoires across multiple human tissues
433 using RNA sequencing. *Nat. Commun.* (2020). doi:10.1038/s41467-020-16857-7
- 434 13. Ghraichy, M., Galson, J. D., Kelly, D. F. & Trück, J. B-cell receptor repertoire sequencing
435 in patients with primary immunodeficiency: a review. 1–16 (2017).
436 doi:10.1111/imm.12865
- 437 14. Galson, J. D., Pollard, A. J., Trück, J. & Kelly, D. F. Studying the antibody repertoire
438 after vaccination: Practical applications. *Trends in Immunology* **35**, 319–331 (2014).
- 439 15. Lindau, P. & Robins, H. S. Advances and applications of immune receptor sequencing
440 in systems immunology. *Curr. Opin. Syst. Biol.* **1**, 62–68 (2017).
- 441 16. Georgiou, G. *et al.* The promise and challenge of high-throughput sequencing of the
442 antibody repertoire. *Nature Biotechnology* **32**, 158–168 (2014).
- 443 17. Berkowska, M. A. *et al.* Human memory B cells originate from three distinct germinal
444 center-dependent and -independent maturation pathways. *Blood* (2011).
445 doi:10.1182/blood-2011-04-345579
- 446 18. Mroczek, E. S. *et al.* Differences in the composition of the human antibody repertoire
447 by b cell subsets in the blood. *Front. Immunol.* (2014). doi:10.3389/fimmu.2014.00096
- 448 19. Galson, J. D. *et al.* BCR repertoire sequencing: Different patterns of B-cell activation
449 after two Meningococcal vaccines. *Immunol. Cell Biol.* **93**, 885–895 (2015).
- 450 20. Wu, Y. C. *et al.* High-throughput immunoglobulin repertoire analysis distinguishes
451 between human IgM memory and switched memory B-cell populations. *Blood* (2010).
452 doi:10.1182/blood-2010-03-275859
- 453 21. Glanville, J. *et al.* Naive antibody gene-segment frequencies are heritable and

454 unaltered by chronic lymphocyte ablation. *Proc. Natl. Acad. Sci.* **108**, 20066–20071
455 (2011).

456 22. Ghraichy, M. *et al.* Maturation of the Human Immunoglobulin Heavy Chain Repertoire
457 With Age. *Front. Immunol.* (2020). doi:10.3389/fimmu.2020.01734

458 23. Jackson, K. J. L., Wang, Y. & Collins, A. M. Human immunoglobulin classes and
459 subclasses show variability in VDJ gene mutation levels. *Immunol. Cell Biol.* (2014).
460 doi:10.1038/icb.2014.44

461 24. Kitaura, K. *et al.* Different somatic hypermutation levels among antibody subclasses
462 disclosed by a new next-generation sequencing-based antibody repertoire analysis.
463 *Front. Immunol.* (2017). doi:10.3389/fimmu.2017.00389

464 25. Vander Heiden, J. A. *et al.* PRESTO: A toolkit for processing high-throughput
465 sequencing raw reads of lymphocyte receptor repertoires. *Bioinformatics* **30**, 1930–
466 1932 (2014).

467 26. Gupta, N. T. *et al.* Change-O: A toolkit for analyzing large-scale B cell immunoglobulin
468 repertoire sequencing data. *Bioinformatics* **31**, 3356–3358 (2015).

469 27. Ye, J., Ma, N., Madden, T. L. & Ostell, J. M. IgBLAST: an immunoglobulin variable
470 domain sequence analysis tool. *Nucleic Acids Res.* **41**, W34–W40 (2013).

471 28. Lunter, G. & Goodson, M. Stampy: A statistical algorithm for sensitive and fast
472 mapping of Illumina sequence reads. *Genome Res.* **21**, 936–939 (2011).

473 29. Yaari, G., Uduman, M. & Kleinsteiner, S. H. Quantifying selection in high-throughput
474 Immunoglobulin sequencing data sets. *Nucleic Acids Res.* **40**, e134–e134 (2012).

475 30. 3.5.1., R. D. C. T. A Language and Environment for Statistical Computing. *R Foundation
476 for Statistical Computing* **2**, <https://www.R-project.org> (2018).

477 31. Venables, W. N. & Ripley, B. D. Modern Applied Statistics with S (fourth.). New York:
478 Springer. *Retrieved from* <http://www.stats.ox.ac.uk/pub/MASS4> (2002).

479 32. Pedregosa, F. *et al.* Scikit-learn: Machine Learning in Python. *J. Mach. Learn. Res.*
480 (2015).

481 33. Bashford-Rogers, R. J. M., Smith, K. G. C. & Thomas, D. C. Antibody repertoire analysis
482 in polygenic autoimmune diseases. *Immunology* **155**, 3–17 (2018).

483 34. Briney, B. S., Willis, J. R., Hicar, M. D., Thomas, J. W. & Crowe, J. E. Frequency and
484 genetic characterization of V(DD)J recombinants in the human peripheral blood
485 antibody repertoire. *Immunology* (2012). doi:10.1111/j.1365-2567.2012.03605.x

486 35. Larimore, K., McCormick, M. W., Robins, H. S. & Greenberg, P. D. Shaping of Human
487 Germline IgH Repertoires Revealed by Deep Sequencing. *J. Immunol.* **189**, 3221–3230
488 (2012).

489 36. DeWitt, W. S. *et al.* A public database of memory and naive B-cell receptor sequences.
490 *PLoS One* (2016). doi:10.1371/journal.pone.0160853

491 37. Bautista, D. *et al.* Differential Expression of IgM and IgD Discriminates Two
492 Subpopulations of Human Circulating IgM+IgD+CD27+ B Cells That Differ
493 Phenotypically, Functionally, and Genetically. *Front. Immunol.* (2020).
494 doi:10.3389/fimmu.2020.00736

495 38. Friedensohn, S. *et al.* Synthetic standards combined with error and bias correction
496 improve the accuracy and quantitative resolution of antibody repertoire sequencing
497 in human naïve and memory B cells. *Front. Immunol.* (2018).
498 doi:10.3389/fimmu.2018.01401

499 39. Briney, B. S., Willis, J. R., McKinney, B. A. & Crowe, J. E. High-throughput antibody
500 sequencing reveals genetic evidence of global regulation of the nave and memory
501 repertoires that extends across individuals. *Genes Immun.* (2012).

502 doi:10.1038/gene.2012.20

503 40. Rubelt, F. *et al.* Individual heritable differences result in unique cell lymphocyte
504 receptor repertoires of naïve and antigen-experienced cells. *Nat. Commun.* (2016).
505 doi:10.1038/ncomms11112

506 41. Greiff, V. *et al.* Learning the High-Dimensional Immunogenomic Features That Predict
507 Public and Private Antibody Repertoires. *J. Immunol.* (2017).
508 doi:10.4049/jimmunol.1700594

509 42. Ostmeyer, J. *et al.* Statistical classifiers for diagnosing disease from immune
510 repertoires: A case study using multiple sclerosis. *BMC Bioinformatics* (2017).
511 doi:10.1186/s12859-017-1814-6

512 43. Konishi, H. *et al.* Capturing the differences between humoral immunity in the normal
513 and tumor environments from repertoire-seq of B-cell receptors using supervised
514 machine learning. *BMC Bioinformatics* (2019). doi:10.1186/s12859-019-2853-y

515 44. Shemesh, O., Polak, P., Lundin, K. E. A., Sollid, L. M. & Yaari, G. Machine Learning
516 Analysis of Naïve B-Cell Receptor Repertoires Stratifies Celiac Disease Patients and
517 Controls. *Front. Immunol.* (2021). doi:10.3389/fimmu.2021.627813

518 45. Wesemann, D. R. *et al.* Immature B cells preferentially switch to IgE with increased
519 direct Sp to Se recombination. *J. Exp. Med.* (2011). doi:10.1084/jem.20111155

520 46. Looney, T. J. *et al.* Human B-cell isotype switching origins of IgE. *J. Allergy Clin.
521 Immunol.* (2016). doi:10.1016/j.jaci.2015.07.014

522 47. Meyts, I., Bossuyt, X., Proesmans, M. & De, B. Isolated IgG3 deficiency in children: To
523 treat or not to treat? Case presentation and review of the literature. *Pediatric Allergy
524 and Immunology* (2006). doi:10.1111/j.1399-3038.2006.00454.x

525 48. IJsspeert, H. *et al.* Evaluation of the Antigen-Experienced B-Cell Receptor Repertoire in
526 Healthy Children and Adults. *Front. Immunol.* **7**, 410 (2016).

527 49. De Jong, B. G. *et al.* Human IgG2- and IgG4-expressing memory B cells display
528 enhanced molecular and phenotypic signs of maturity and accumulate with age.
529 *Immunol. Cell Biol.* (2017). doi:10.1038/icb.2017.43

530

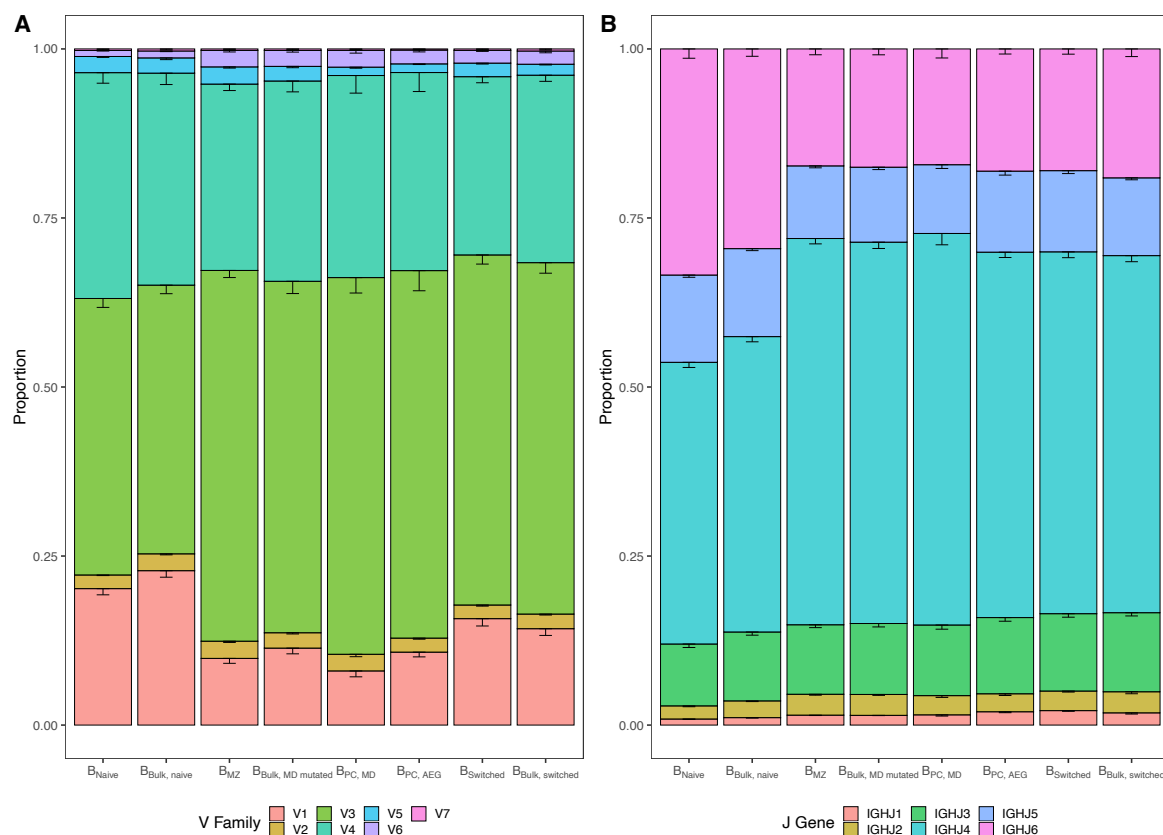
531 **Supplementary material**

532

533 **Supplementary table 1:**

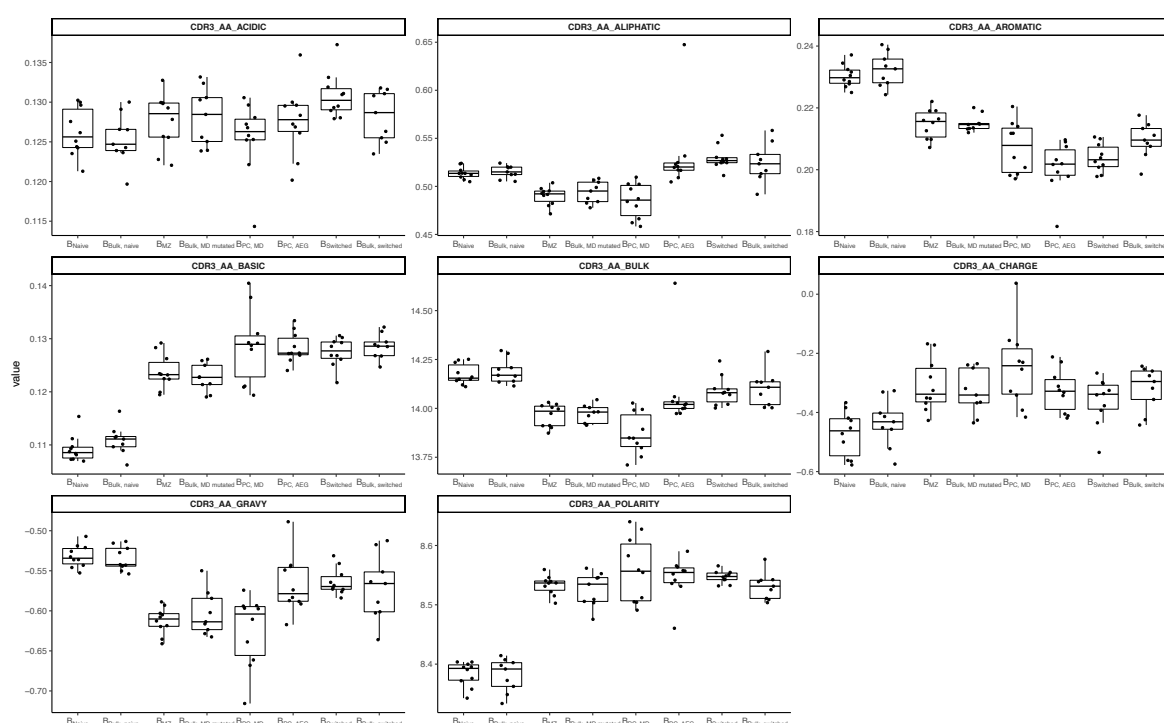
Participant ID	Cells	Age	Sex	B cell number	Purity
Co C.081.1 BC	MZB	50	M	250000	93.6
Co C.081.1 BC	Naive	50	M	250000	96.7
Co C.080.1 BC	MZB	NA	M	250000	NA
Co C.080.1 BC	Naive	NA	M	250000	NA
Co C.082.1 BC	Naive	40	M	250000	97.6
Co C.083.1 BC	MZB	18	M	250000	82.9
Co C.083.1 BC	Naive	18	M	250000	98.2
Co C.084.1 BC	MZB	36	F	250000	86.4
Co C.084.1 BC	Naive	36	F	250000	96.7
Co C.081.1 BC	Swt	50	M	250000	98.8
Co C.080.1 BC	Swt	NA		250000	NA
Co C.080.1 BC	PC	NA		55000	NA
Co C.081.1 BC	PC	50	M	1.00E+05	45.8
Co C.082.1 BC	MZB	40	M	250000	81.5
Co C.082.1 BC	Swt	40	M	250000	98.7
Co C.082.1 BC	PC	40	M	19000	67.8
Co C.083.1 BC	Swt	18	M	250000	99.2
Co C.083.1 BC	PC	18	M	21000	32.8
Co C.081.1 BC	CD19	50	M	5.00E+05	NA
Co C.084.1 BC	Swt	36	F	250000	98.2
Co C.084.1 BC	PC	36	F	15000	30.3
Co C.084.1 BC	CD19	36	F	5.00E+05	NA
Co C.085.1 BC	CD19	41	M	5.00E+05	NA
Co C.085.1 BC	PC	41	M	21000	32.2
Co C.085.1 BC	Swt	41	M	250000	97.5
Co C.085.1 BC	Naive	41	M	250000	98.9
Co C.085.1 BC	MZB	41	M	250000	92.1
Co BC7 BC	Naive	49	F	250000	93.6
Co BC8 BC	MZB	59	F	250000	90.5
Co BC8 BC	Naive	59	F	250000	95.2
Co BC9 BC	MZB	44	F	250000	91.8
Co BC9 BC	Naive	44	F	250000	99.2
Co BC10 BC	MZB	51	F	250000	94.2
Co BC10 BC	Naive	51	F	250000	96.2
Co BC7 BC	CD19	49	F	5.00E+05	NA
Co BC7 BC	Swt	49	F	250000	95.6
Co BC7 BC	PC	49	F	14000	37
Co BC8 BC	CD19	59	F	5.00E+05	NA
Co BC8 BC	Swt	59	F	250000	97.3
Co BC8 BC	PC	59	F	24000	68.2
Co BC9 BC	CD19	44	F	5.00E+05	NA
Co BC9 BC	Swt	44	F	250000	94.5
Co BC9 BC	PC	44	F	22000	82.8
Co BC10 BC	CD19	51	F	5.00E+05	NA
Co BC10 BC	Swt	51	F	250000	99.1
Co BC10 BC	PC	51	F	19000	60
Co C.082.1 BC	CD19	40	M	5.00E+05	NA
Co BC7 BC	MZB	49	F	250000	86.7
Co C.083.1 BC	CD19	18	M	5.00E+05	NA

534



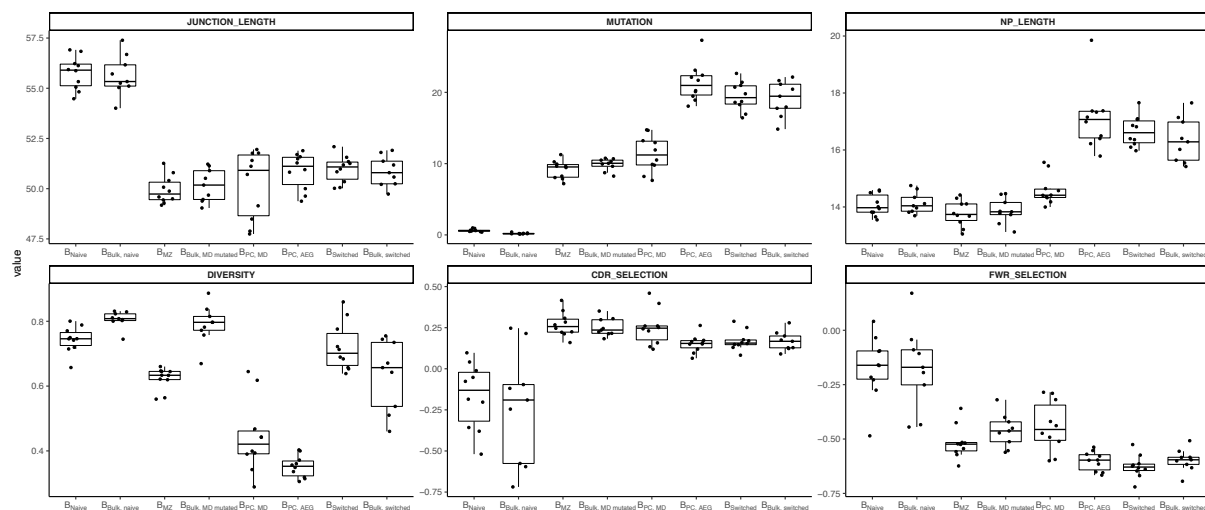
535
536
537
538
539

Supplementary figure 1 A) V family and B) J gene usage by B cell subpopulation. Bar plots indicate the proportion of sequences with a certain gene. Error bars represent the standard error of the mean.



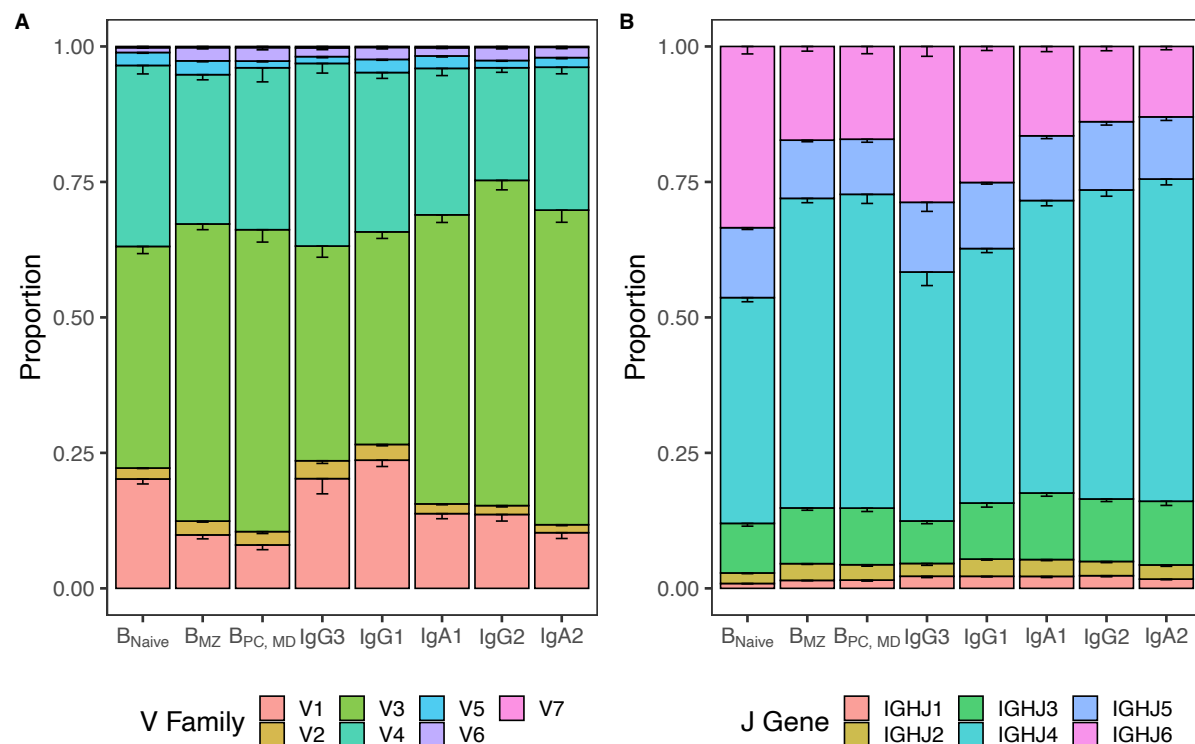
540
541
542

Supplementary figure 2 : Comparison of CDR3 amino acid physiochemical properties in different B cell subpopulations.



543
544
545
546

Supplementary figure 3 : Comparison of global repertoire metrics in different B cell subpopulations.



547
548
549
550

Supplementary figure 4: A) V family and B) J gene usage in different B cell subpopulations and isotype subclasses. Bar plots indicate the proportion of sequences with a certain gene. Error bars represent the standard error of the mean.